Development of enhanced double-sided 3D radiation sensors for pixel detector upgrades at HL-LHC

Marco Povoli[1]

[1] Dipartimento di Ingegneria e Scienza dell'Informazione
University of Trento, Italy

Trento, Italy - February 20, 2012

[Work supported by INFN CSN V, projects "TREDI" (2005-2008) and "TRIDEAS" (2009-2011)]

Outline

The Large Hadron Collider (LHC)

The Large Hadron Collider (LHC)

- Largest particle collider ever built
- Near Geneva, underneath the swiss/french border
- Total ring length of about 27 Km
- First started in 2008
- The official physics program started in 2009

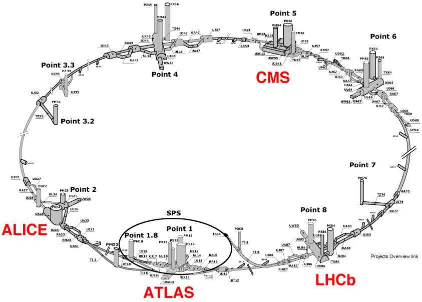

Basic machine parameters

- Proton or Lead Ion collisions
- Nominal proton energy of 7 TeV (per beam)
- Bunch spacing of 25 ns
- Design luminosity 10^{34} cm^{-2}s^{-1}

Physics program

- Discovery of new particles/theories
- Particles collide inside the four experiments
- ATLAS and CMS: general purpose
- ALICE: study lead ions collision
- LHCb: specialized in b-physics

General purpose experiments
A Toroidal LHC ApparatuS (ATLAS)

Basic parameters

- 45 meters long
- 25 meters in diameter
- weights about 7000 tons

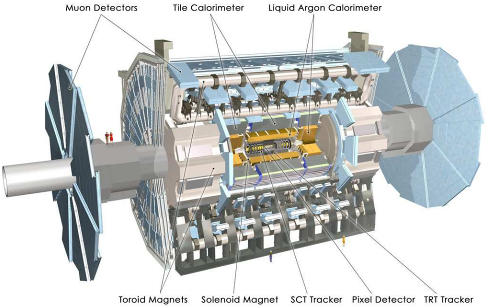

Structure (inside-out)

1. Inner detector
2. Calorimeters
3. 2 Tesla solenoid magnets
4. Muon spectrometers

The inner detector

- Several layers of silicon detectors and one layer of straw tube detectors
- Needed to reconstruct the particle interaction point
- Required to be very fast
- Operates in extremely harsh conditions

The current ATLAS silicon tracker

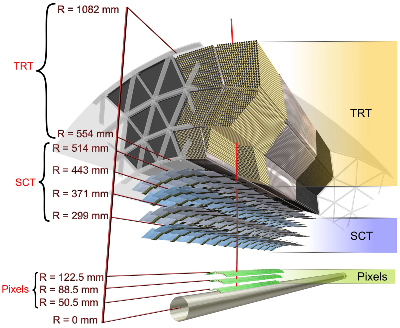

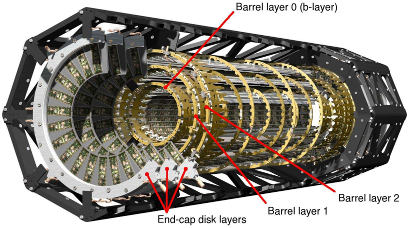

Barrel cross-section

- Total radius of roughly 1 m
- Pixel detector: 3 layers of **n-in-n pixel sensors**
- Strip detector: 4 layers of **p-in-n strip sensors**
- Transition Radiation Tracker: straw tubes interleaved with scintillating fibers

The pixel detector

- Three barrel layers at radiuses 50.5, 88.5, 122.5 mm
- 6 end-caps (three on each side)
- Pixel size 50×400 μm^2
- Covers an area of $\sim$1.7 m^2
- Approximately 67 million channels
- **Designed to withstand a fluence of 1×10^{15} 1 MeV n_{eq} cm^{-2}**

The ATLAS Insertable B-Layer (IBL)

Planned installation during the first long shutdown (2013-2014)

CURRENT PIXEL DETECTOR

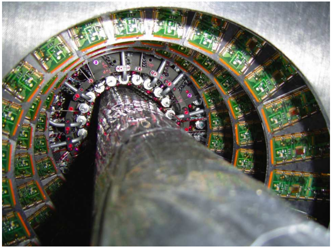

RENDERING OF THE IBL

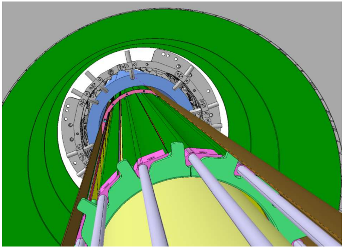

Addition of a fourth pixel layer close to the beam pipe

Motivations

- Maintain the event pile-up under control as LHC luminosity increases
- Add redundancy to recover partial failure of modules in the other pixel layers
- Increase tracking and reconstruction accuracy

Main design parameters

- Need to reduce the beam pipe radius by 4mm
- Placed at 33.25 mm from the center of the beam pipe
- Will need to withstand a fluence of $\mathbf{5 \times 10^{15}\ n_{eq}\ cm^{-2}}$

[M. Capeans, (The ATLAS Collaboration), ATLAS-TDR-019]

The ATLAS Insertable B-Layer (IBL)

Sensor requirements

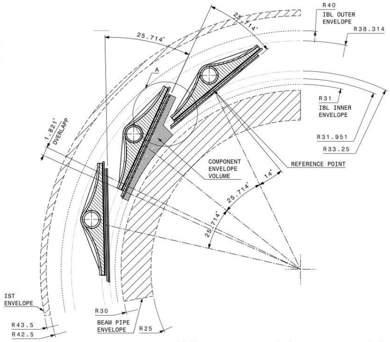

Parameter	Value	unit
Total number of staves	14	-
Pixel size (Φ, z)	**50, 250**	μm
Dead edge extension	**200**	μm
Sensor thickness	$<$250	μm
NIEL dose tolerance	**5×10^{15}**	n_{eq}/cm^2
Hit efficiency in active area	**>97%**	-
Operating bias voltage	**<1000**	V
Operating temperature	-15	$^\circ$C

- Reduced pixel size in the *z* direction (250 μm) to increase the spatial resolution
- No tilt possible in the *z* direction $\rightarrow$ need for reduced dead area at the edges

[A. Clark, et al., (The ATLAS IBL collaboration), (2012) JINST 7 P11010]

NEED FOR ADVANCED RADIATION HARD DETECTORS

Radiation damage in silicon (summary)

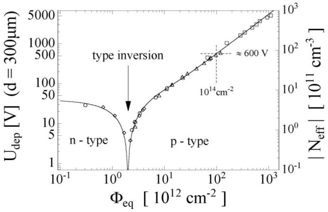

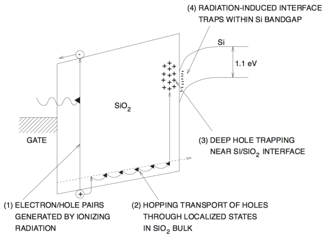

Bulk damage

- Due to **Non Ionizing Energy Loss (NIEL)**
- Displacement of atoms in the Silicon lattice
- Built-up of crystal defects

Consequences

- Change in effective doping concentration (higher depletion, under-depletion)
- Increase of leakage current (shot noise, thermal runaway)
- Increase of charge trapping (charge losses)

Surface damage

- Due to **Ionizing Energy Loss (IEL)**
- Radiation generates carriers in SiO_2
- Electrons can escape while holes get trapped at the Si/SiO_2 interface

Consequences

- Accumulation of charge at the SiO_2/Si interface (inter-pixel capacitance and isolation and breakdown behavior)
- Increased charge trapping at the Si/SiO_2
- Increased surface recombination velocity

LOWERING OF THE S/N RATIO!

[Michael Moll - MC-PAD Network Training, Ljubljana, 27.9.2010]

Countermeasures

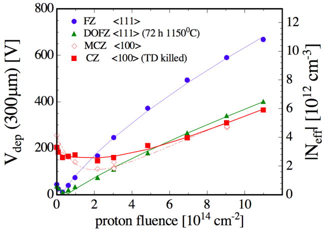

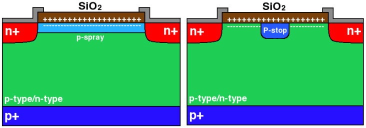

Surface isolation

- Important to assure inter-electrode isolation
- Typically achieved using p-spray, p-stop or a combination of the two

Material engineering

Deliberate incorporation of impurities or defects into the silicon bulk to improve radiation tolerance of the detectors

- Oxygen rich Silicon (FZ, DOFZ, Cz, MCZ)
- Pre-irradiated Silicon

New Materials

- Silicon carbide (SiC)
- Amorphous Silicon
- Diamond

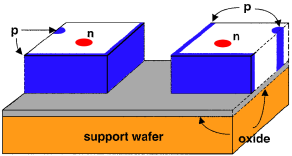

Device engineering

- p-type silicon detectors (n-in-p)
- Thin detectors
- **3D detectors**

[Michael Moll - MC-PAD Network Training, Ljubljana, 27.9.2010]

Full 3D detectors

Original idea - PROS and CONS

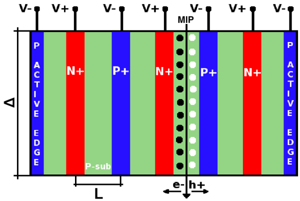

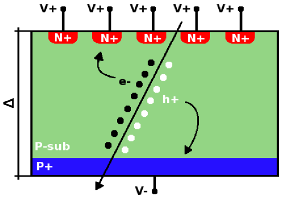

Features of 3D detectors

- First proposed by S. Parker and collaborators in the mid '90s *[NIMA 395 (1997), 328]*
- Decouple the active volume from the inter-electrode distance
- Low full depletion voltage ($<$**10 V**)
- Short collection distances ($\sim$**50** μ**m**)
- Low trapping probability after irradiation
- Small dead area along the edges

Disadvantages of 3D detectors

- Columns are partially dead regions
- Non uniform response (low field regions are present)
- Higher capacitance (higher noise)
- Fabrication process complex and more expensive

The ATLAS 3D sensor collaboration

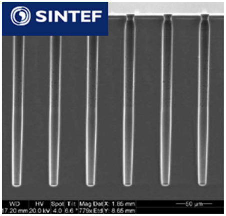

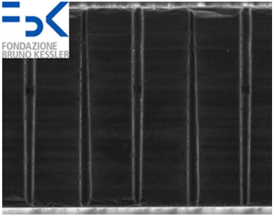

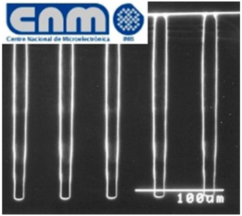

Institutes and processing facilities

- 18 Institutes
- 4 processing facilities:
  - SNF (Stanford, USA)
  - SINTEF (Oslo, Norway)
  - CNM (Barcelona, Spain)
  - FBK (Trento, Italy)

Available 3D technologies

- Full 3D with active-edges (SNF and SINTEF)
- 3D-DDTC with slim-edges (FBK, CNM)
- <u>Full</u> 3D-DDTC with slim-edges (FBK)

Main targets

1. Speed-up the test and industrialization of 3D silicon sensors
2. Production and testing of 3D sensors for the IBL

[C. Da Vià, et al., NIMA694 (2012), 321]

3D technology for the IBL developed at FBK

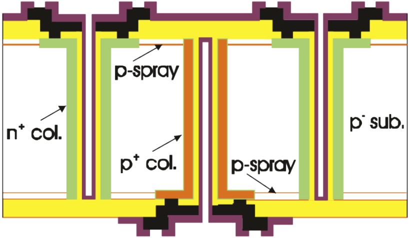

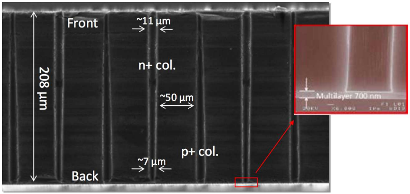

Main geometrical features

- Double-type column approach
- Fully double-sided
- Columns etched from both wafer sides
- Fully passing through columns
- Empty electrodes (no polysilicon filling)
- Surface isolation by means on p-spray implantations on both wafer sides

SEM cross-section

- Very good etching uniformity
- Columns are all passing through
- Slight shrinking of the column tip (not affecting device behavior)

[G. Giacomini, et al., to appear in IEEE TNS (2013)]

3D technology for the IBL developed at FBK

The common wafer layout and pixel layout

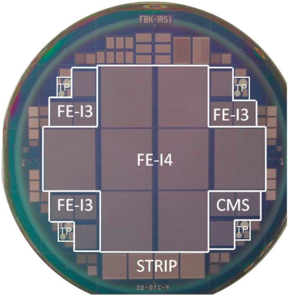

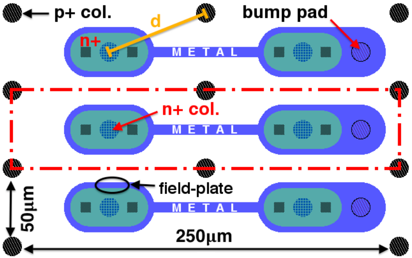

$\longrightarrow$ z direction

Common wafer layout

- 4 inches wafers
- 8 ATLAS FE-I4 pixel detectors
- 9 FE-I3 pixel detectors
- 3 CMS pixel detectors
- 4 strip detectors (80 µm pitch)
- Several planar and 3D test structures

Single pixel layout

- Pixel size: 50×250 µm^2
- 2E configuration: 2 n^+ columns per pixel
- Inter-electrode distance (d): $\sim$67 µm
- With field-plate

[C. Da Vià, et al., NIMA694 (2012), 321]

Motivation for FE-I4 pixel layout

Results from previous technologies

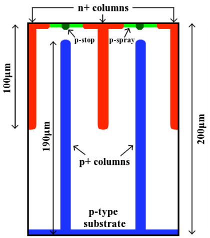

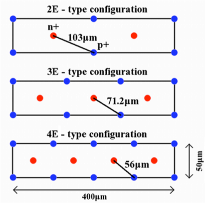

Previous 3D-DDTC technology at FBK

- Non-passing through columns
- Pixel size $50 \times 400\ \mu m^2$ (FE-I3)
- Three pixel layouts (2E, 3E, 4E)

Best performances from 3E devices (71 μm)

- Noise $\sim$205 e^-
- Good CCE up to $1 \times 10^{15}\ n_{eq}/cm^2$
- Tracking efficiency $>$98% at $1 \times 10^{15}\ n_{eq}/cm^2$

$\Phi_{eq} = 1 \times 10^{15}\ n_{eq}/cm^2$

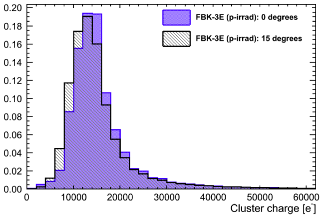

[A. Micelli, NIMA650 (2011), 150]

$\Phi_{eq} = 1 \times 10^{15}\ n_{eq}/cm^2$

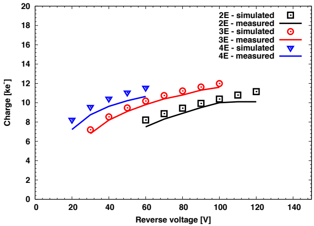

[A. La Rosa, NIMA681 (2012), 25]

Edge termination (SLIM-EDGE)
Motivation and design

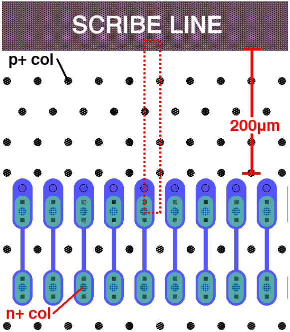

Slim-edges in the *z* direction

- Requirement: ⩽200 µm in the beam (z) direction
- Motivation: not possible to tilt modules in the z direction due to space constrains
- Fence of ohmic columns to prevent the depletion region to reach the scribe line
- Designed with the aid of numerical simulations

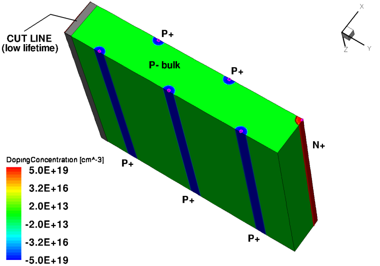

Computer aided design

- Simulation of a structure including the last junction column and the ohmic fence
- Simulation domain highlighted with the dashed rectangle
- Scribe line model with a low lifetime region (<1 ns)
- Monitor the current of the last junction column
- No avalanche models

Edge termination (SLIM-EDGE)

Motivation and design

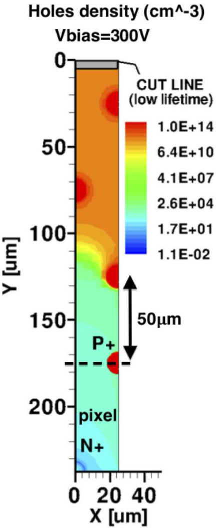

[M. Povoli, et al., JINST 7 (2012) C01015]

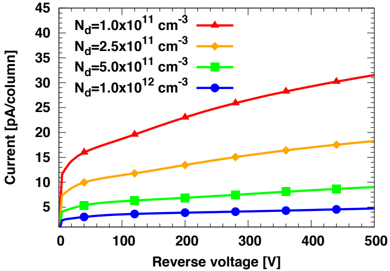

[G.-F. Dalla Betta, et al., NSS10 Conf. Record, pp. 382-387]

Simulation results

- Different bulk doping concentrations tested
- No signs of current increase up to 500 V (well above expected operation voltage)
- The depletion region extends outside the active area by about 75 µm at 300 V
- Safe device operation with a 200 µm slim-edge
- **Note: conservative design!**

On wafer selection

Motivation and procedure

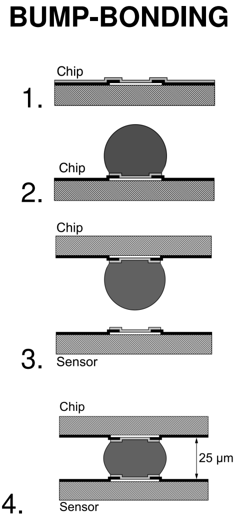

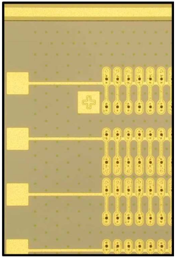

[G. Giacomini, et al., to appear in IEEE TNS (2013)]

On-wafer sensor selection

- **The bump-bonding is complex and very expensive**
- Assemble **only** good sensor tiles
- Wafer with more than 3 good sensors are sent for bump-bonding

Temporary metal layer

- Deposited on top of the frontside passivation
- Strip-like metalization
- 80 strips connecting 336 pixels each
- Automatic current measurements
- The sum of all strip currents gives the total sensor current

On wafer selection

Example test results

GOOD WAFER (ATLAS12)

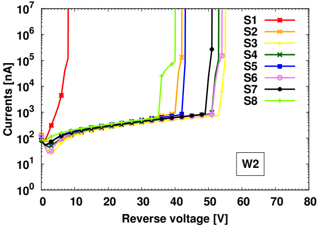

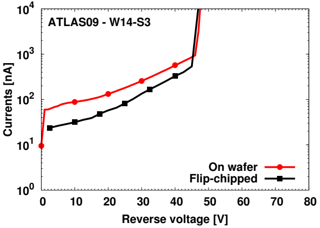

[C. Da Vià, et al., NIMA694 (2012), 321]

Parameter	Symbol	Value
Operation temperature	T_{op}	20-24 °C
Depletion voltage	V_{depl}	$<$15 V
Operation voltage	V_{op}	$\geqslant V_{depl}$+10 V
Leakage current at V_{op}	**$I(V_{op})$**	**$<$2 μA**
Breakdown voltage	**V_{bd}**	**$>$25 V**
Current "slope"	$I(V_{op})/I(V_{op}-5V)$	$<$2

Wafer/sensor selection

- Good sensors always have currents much lower than the set limit
- Breakdown voltages are typically higher than 30 V for good detectors
- Confirmation of the selection method comparing current pre/after bump-bonding
- **Yield of IBL production at FBK: 56.82%**

NOTE: further investigation needed on some aspects

- The breakdown is lower than for standard planar detectors (can be critical after irradiation)
- In some cases the behavior is not very uniform
- Necessary to perform a thorough electrical characterization

Detailed electrical characterization

3D diodes

FE-I4 with field-plate

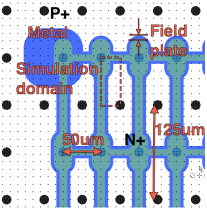

FE-I4

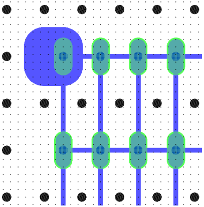

80 µm pitch

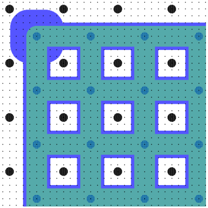

CMS - 1E

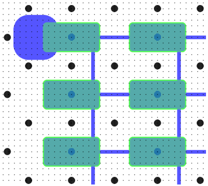

3D diode

- Two terminal device having an area of roughly 10 mm^2
- Electrodes of the same type are shorted together
- All the geometries of larger detectors are reproduced
- Eases the characterization

Performed tests

- I-V and C-V measurements as a function of the temperature
- Numerical simulations to confirm the findings and gain a deeper understanding of the device behavior

FE-I4 (backside)

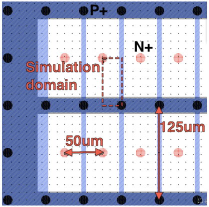

[M. Povoli, et al., NIMA699, (2013), 22]

IV measurements with variable temperature

IV Curves

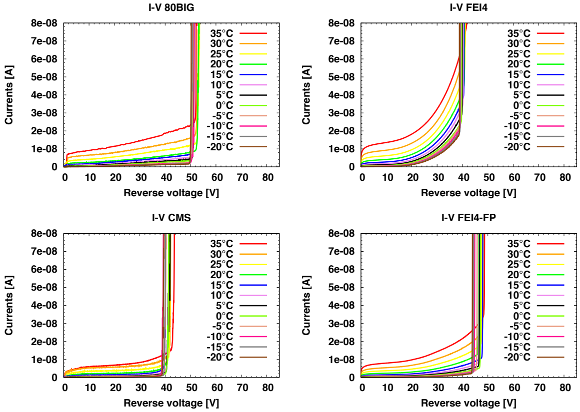

Setup

- Devices coming from wafer W20 of the ATLAS09 batch
- Devices were diced and wire bonded on small PCBs
- Wire bonding contribution is negligible
- Temperature variation between $-20^\circ C$ and $35^\circ C$ inside a climatic chamber
- Measurements performed with HP4145

Preliminary results

- Each type of device has its own characteristic behavior
- Breakdown voltages between 40 and 50V
- Different current slope for different devices
- More details in the next slide...

Data analysis

Intrinsic electric behavior

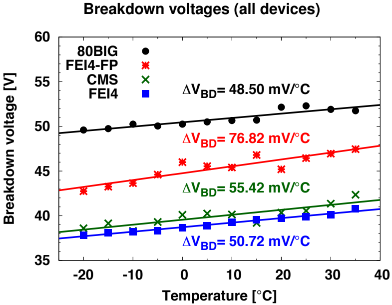

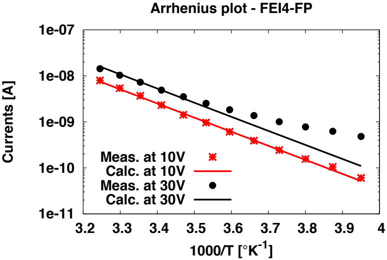

Breakdown voltages

- Breakdown between 40 and 50V
- Linear increase with temperature
- The increase is between $\sim$ 50 and $\sim 80 mV/^\circ C$
- In agreement with the expectation

[Crowell, C. R. and S. M. Sze, Appl. Phys. Lett. 9, 6 (1966) 242-244.]

Purpose

Distinction between thermal and avalanche generation

Equation

$$I(T) = I(T_R)\left(\frac{T}{T_R}\right)^2 \exp\left[\frac{E}{2k_B}\left(\frac{1}{T_R} - \frac{1}{T}\right)\right]$$

Results

- T_R=293.15 °K
- Very good agreement at low biases
- The agreement is lost as breakdown approaches

Investigation through numerical simulations

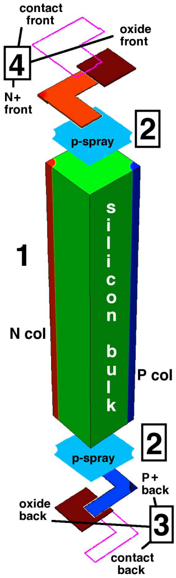

Simulated structure

- A quarter of elementary cell (thanks to symmetry)
- Bulk doping: 7×10^{11} cm^{-3} (p-type, measured)
- One columnar electrode per type
- Measured p-spray profiles
- Measured n^{+} and p^{+} surface implantations
- Device layout fully reproduced

Incremental addition of the layout details

- Used to estimate the contribution of each component of the device capacitance
- Allows discriminate between inter-electrode and surface capacitance

Simulation of the full structure

- Estimation of the expected breakdown voltage and current levels
- Analysis of the distribution of electrical quantities (e.g. Electric field and Electrostatic potential)

C-V measurements vs. C-V simulations

FE-I4 diode with field-plate

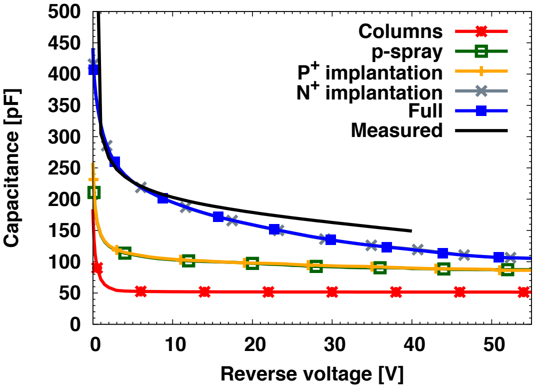

Results

- Electrodes contribution: $\sim$ **51.4pF** (constant)
- **p-spray** causes an **increase** of $\sim$ **30pF** (basically constant)
- P^+ implantation and metal on the back side **do not** cause much increase
- N^+ implantation and metal on the front side cause an increase of $\sim$ **63pF** at a bias voltage of **20V**
- At higher biases the contribution of front side saturates to a value similar to the one obtained only with electrodes and p-spray ($\sim$ **103pF**)
- Measured capacitance does not fully saturate at 40V (instrument limitations)

Distribution of electrical quantities

FE-I4 diode - Electric field

FE-I4 with FP

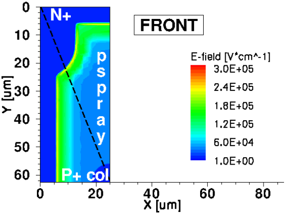

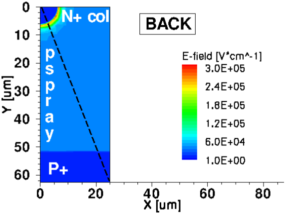

FE-I4

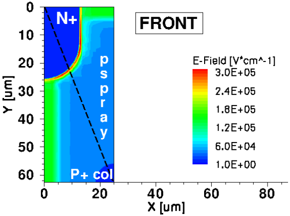

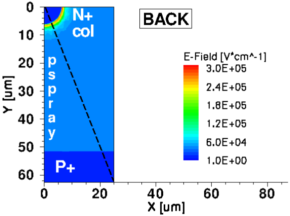

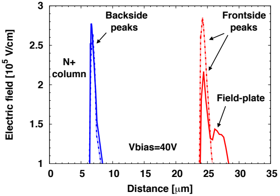

- Large field peaks on both the upper and lower surfaces
- Peaks are placed at the n^{+} to p-spray junction
- Particularly critical due to the high dose p-spray implantation
- Both structures have similar field-peaks on the backside
- The field-plate redistributes and lowers the field on the frontside

Front-side surface irradiation

X-Rays - 2 Mrad (60 minutes irradiation)

P-spray compensation to increase the breakdown voltage
How large is the increase?

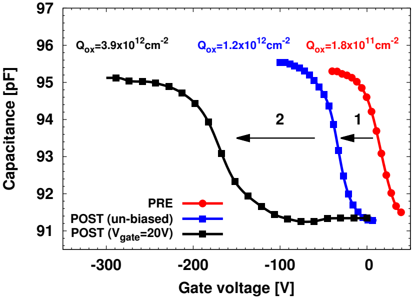

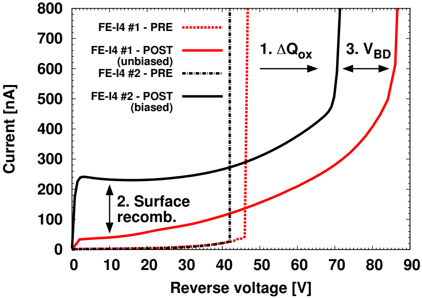

- Irradiation performed at "Laboratori Nazionali di Legnaro" *(LNL, Padova, Italy, thanks to Serena Mattiazzo)*
- Use of MOS capacitors to monitor the increase in oxide charge
- Two irradiations: without and with bias (20 V)
- Considerably larger charge when irradiation is performed under bias

- Two different FE-I4 diodes with field-plate
- Current increase do to surface generation
- Limited breakdown increase
- Pre-irradiation trend maintained after
- **Confirm that the breakdown occurs on the backside**

Functional characterization of FE-I4 pixel detectors

Readout chip and measurement setups

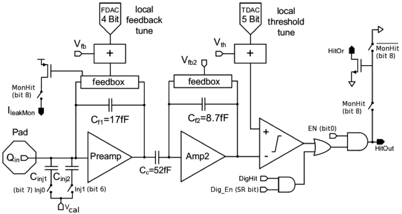

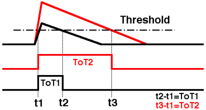

[A. Clark, et al., (The ATLAS IBL collaboration), (2012) JINST 7 P11010]

ATLAS FE-I4 readout chip

- Designed to withstand a TID of 250 Mrad
- Leakage compensation
- Double stage charge amplifier with constant current discharge
- Discriminator after charge amplifier
- Operates in **Time Over Threshold (ToT)** mode
- The ToT is representative of the collected charge

The USBPix system

[http://icwiki.physik.uni-bonn.de/twiki/bin/view/Systems/UsbPix]

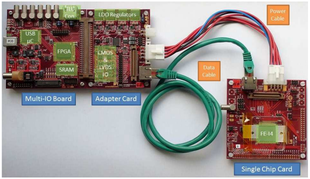

The EUDET Telescope

[D. Haas, EUDET-Report-2007-07]

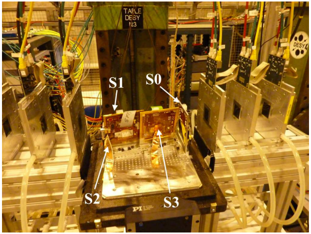

Functional characterization of FE-I4 pixel detectors

Radioactive source scans (^{90}Sr, Lab)

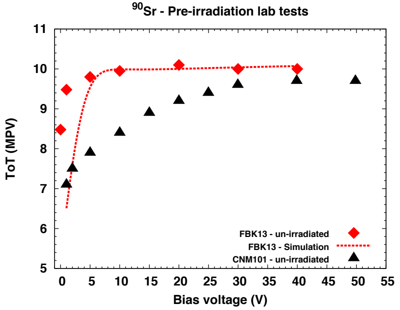

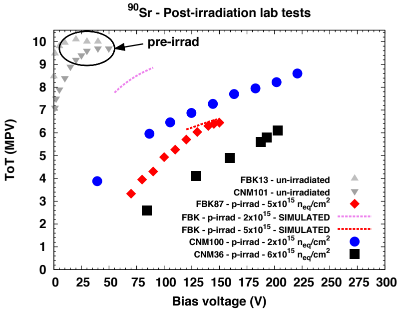

PRE-irradiation

- Comparison between FBK and CNM detectors
- Calibration: 10 ToT at 20 ke^{-}
- Most Probable Value of the "all-cluster" charge distribution
- FBK $\rightarrow$ charge saturation before 10 V
- CNM $\rightarrow$ charge saturation at roughly 25 V
- Numerical simulations (dashed line) confirm the measurement results

POST-irradiation

- Lowering of charge collection due to trapping
- FBK detector irradiated at 5×10^{15} n_{eq}/cm^2 (red) shows a hint of charge saturation at roughly 150 V
- Confirmed by numerical simulations (red dashed line)
- Measurement not available for 2×10^{15} n_{eq}/cm^2 but simulations can be trusted (violet dashed line)
- **Satisfactory performances**

[G.-F. Dalla Betta, et al., VERTEX2012, submitted to POS]

Functional characterization of FE-I4 pixel detectors

Test-beam results (tracking efficiency)

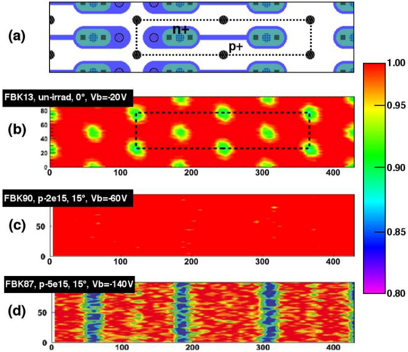

[P. Grenier, et al., "IBL TestBeam Results", presented at the IBL Sensor Review, CERN, 4-5 July 2011]

Beam tests during 2011-2012

- CERN - SPS: 120 GeV pions
- DESY: 4 GeV positrons
- EUDET Telescope
- Both un-irradiated and irradiated samples
- IBL operating conditions
- Planar sensor always used as reference

(b) PRE-irrad. efficiency map

- Good tracking efficiency (98.8%)
- Electrodes appear as less efficient regions
- Possible to obtain higher efficiency by tilting the device with respect to the beam

(c,d) POST-irrad. efficiency map

- FBK90 (2×10^{15} n_{eq}/cm^2) shows great efficiency (99.2%) at 60 V of bias when tilted by 15°
- FBK87 (5×10^{15} n_{eq}/cm^2) exhibits not sufficient efficiency (95.6%) at the chosen bias (140 V)
- **NOTE: when the proper bias is used (e.g. 160 V) the efficiency is back within IBL requirements (98.2%)**

Proton irradiated 3D diodes

80µm pitch

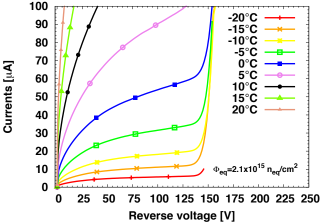

FE-I4

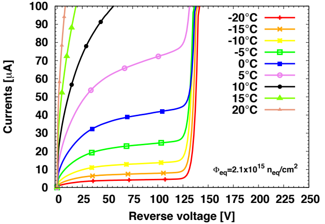

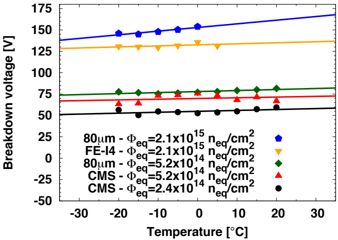

- Irradiation performed at Los Alamos with 800 MeV protons *(thanks to Martin Hoeferkamp)*
- Only half of the requested fluence was delivered
- Increase in breakdown between few volts and ~100 V

Important!

- Devices were selected prior to irradiation
- The FE-I4 diode irradiated at 2×10^{15} n_{eq}/cm^2 shows a breakdown voltage of roughly 125 V
- **A proper sensor selection will assure optimal operating voltages after irradiation!**

SLIM-EDGE characterization

Electrical tests

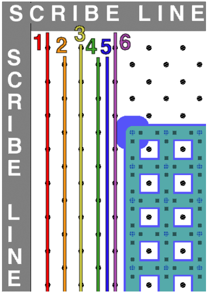

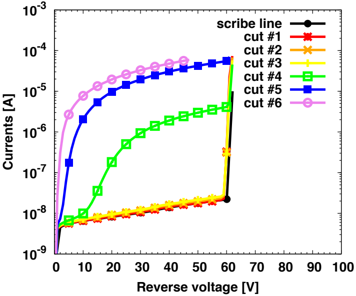

Performed test

- Several cuts performed by means of a diamond saw
- Each cut is closer to the active area
- I-V measurement after each cut

[M. Povoli, et al., JINST 7 (2012) C01015]

Results

- Intrinsic device behavior is equal to roughly 60 V
- No increase in reverse current up to the fourth cut
- Possible to reduce the total edge extension to roughly 100 μm
- **NOTE: critical only before irradiation**

Laser scan V_b=15 V

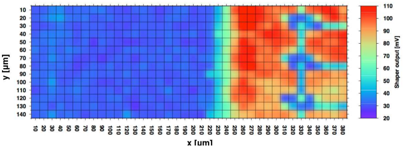

Layout

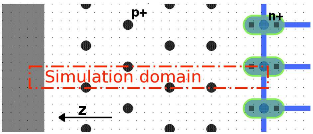

Numerical simulation

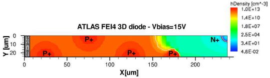

[M. Povoli, et al., JINST 7 (2012) C01015]

Edge efficiency
(Test beam data, $2 \times 10^{15}\ n_{eq}/cm^2$)

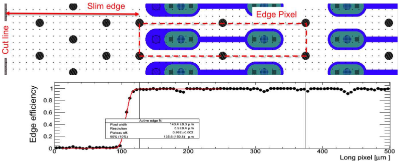

[G.-F. Dalla Betta, et al., VERTEX2012, submitted to POS]

Laser scan (Lab)

- Laser: λ=1060 nm
- Readout: CSA + 20 ns shaper
- Very good agreement with simulations

Edge efficiency after irradiation (test beam)

- Full efficiency inside the active-area
- Roughly 25 µm of the slim-edge are active

Possible technological improvements

Investigation through numerical simulations

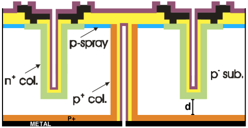

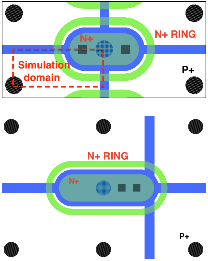

[M. Povoli, et al., IEEE NSS12 Conf. Record, pp. 1334-1338]

- The high field region on the backside can be critical!
- It is of paramount importance to use large operating voltages!
- Lifting the n$^+$ column tip will eliminate the critical region on the backside
- At the same time the fabrication will be easier and faster

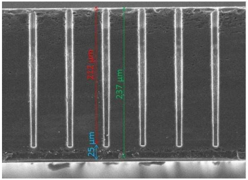

- Important to also improve the field distribution on the frontside
- The field-plate is important
- Some of the designed structures include a floating n$^+$ ring which is intended to interrupt the electrostatic potential of the p-spray
- **The design is performed by means of numerical simulations**

Simulation results

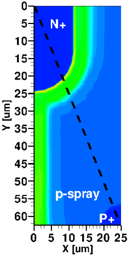

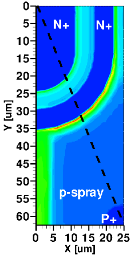

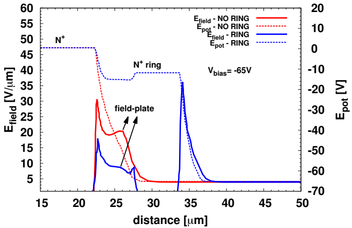

Effect of the floating ring

- The potential of the inner p-spray is lower
- The field at the main junction is lower and the field-plate works properly
- Large peak on the outer ring junction → **causes breakdown**
- The ring placement is critical due to space constrains

Simulated I-Vs

- All devices show larger breakdown than in the previous technology
- The floating ring limits the performances but could act as additional shielding from surface currents
- Raising the n^+ column should deliver breakdown voltages larger than 100 V

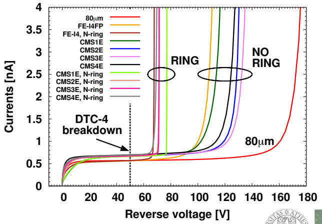

New SLIM-EDGE implementation

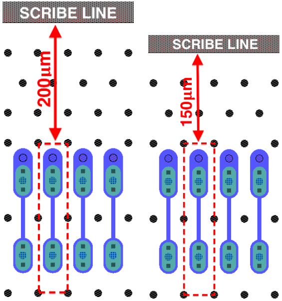

Pixel detectors slim-edge

- Reduced by 50 μm following the indications obtain from previous tests
- Conservative design to avoid problems

New slim-edge implementation for some 3D diodes

- Double row of short trenches (mimicking the active-edge)
- Dead area of roughly 50μm
- Maintains the mechanical integrity and does not require support wafer
- Simulation results at 50 V of bias show how this solutions does not allow the depletion region to reach the scribe line

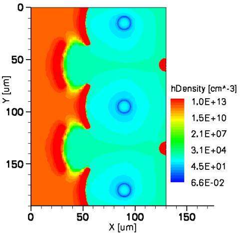

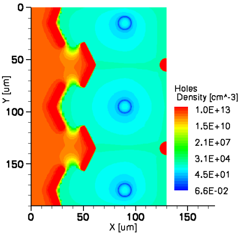

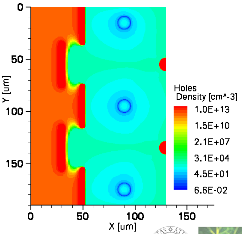

[G.-F. Dalla Betta, et al., NSS11 Conf. Record, pp. 1334-1340]

Fabricated devices
Preliminary electrical characterization

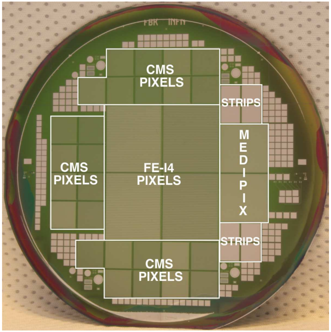

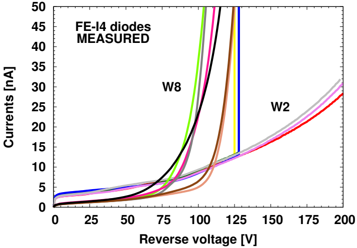

Available devices

- 4 FE-I4 pixel detectors (2 versions)
- 26 CMS pixel detectors (8 versions)
- 2 MEDIPIX-II detectors
- 3D diodes in several different flavors

Preliminary results

- Batch completed in mid October 2012
- A few IV measurements on 3D diodes here reported
- Leakage current higher than expected but acceptable
- Sizable increase of breakdown voltage

[M. Povoli, et al., IEEE NSS12 Conf. Record, pp. 1334-1338]

The ATLAS Forward Physics (AFP)

Motivation and requirements

- Measure protons scattered from the collision
- Located at roughly 200 m both upstreams and downstreams
- Requires reduced edge extension
- FE-I4 modules are investigated

[The ATLAS Collaboration, CERN-LHCC-2011-012]

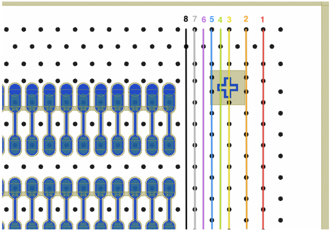

Performed tests

- The edge of interest is the one not "IBL-like"
- Same cut and measure tests were performed
- Proper operation up to the 6th cut (75 μm edge)

Aspect to investigate...

- Very un-uniform irradiation
- Tests are being performed on CNM devices

[S. Grinstein, RESMDD12, submitted to NIMA]

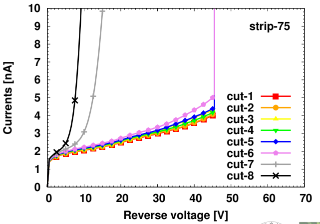

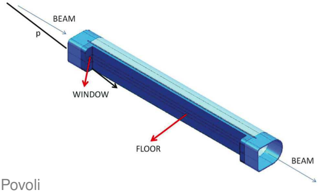

Standard vs. Active Edge detectors

Standard detectors

- In standard detectors a dead border region must be present
- In a good design cracks and damages on the edges should be at least at a few hundreds of micrometers away from the depleted region
- Total dead region $\mathbf{a} + \mathbf{d} \geqslant \mathbf{500}\,\mu\mathbf{m}$

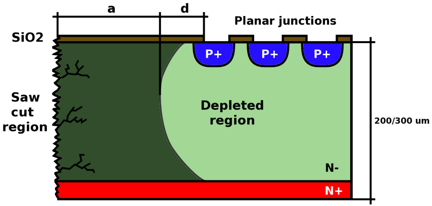

How to limit dead region?

- Cut lines not sawed but etched with Deep Reactive Ion Etching (DRIE) and doped

[C. Kenney, et al., IEEE TNS 48-6 (2001) 2405]

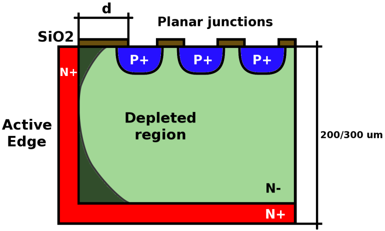

[M. Povoli, NIMA658 (2011), 103]

Problems

- Process is more complicated
- Need for support wafer
- Finding the correct **"d"** to limit early break-down phenomena

Planar detectors with active-edges

Device and wafer layout

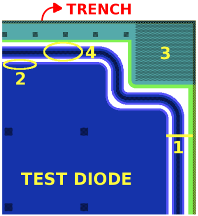

Single-sided p-in-n devices (support wafer)

General device layout (test diode)

1. Distance between n^+ and p^+ doping (GAP)
2. Field-plate
3. Bias pad (connected to the doped trench)
4. Floating p^+ ring

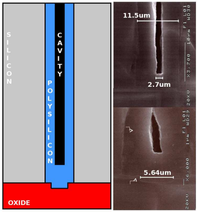

Trench etching

- Designed to be 4 μm
- Not well defined at first
- Optimized etching in the second part of the batch (roughly 10 μm width)
- Partial polysilicon filling needed to restore the surface planarity

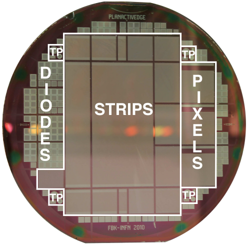

Wafer layout

- Strip detectors with inter-strip pitches of 50, 80 and 100 μm (AC or DC coupled)
- Pixel detectors compatible with the readout chips of the ALICE experiment
- Several test diodes in many different flavors
- Standard planar test structures

Planar detectors with active-edges

Electrical and functional characterization

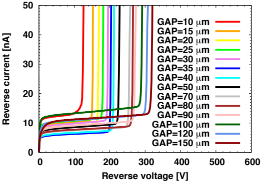

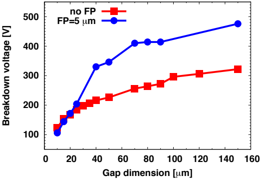

[G.-F. Dalla Betta, et al., NSS11 Conf. Record, pp. 1334-1340]

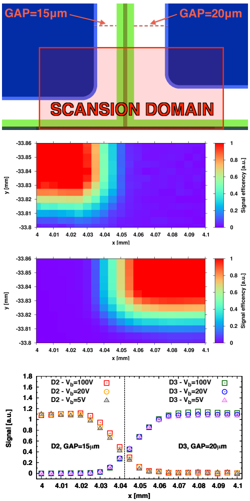

[M. Povoli, et al., NIMA (2012) http://dx.doi.org/10.1016/j.nima.2012.09.035]

Electrical characterization (I-V)

- Good reverse current values and uniformity
- Clear trend with GAP size
- Once again the field-plate proves its effectiveness

Functional tests

- Bi-dimensional X-Ray scan performed at Diamond Light Source, Didcot, UK.
- 15 keV X-rays, spot size ~3 µm FWHM
- Very good signal efficiency up to less than 20 µm away from the edge

Thin 3D detectors with built-in charge multiplication

Evidence and exploitation of this effect

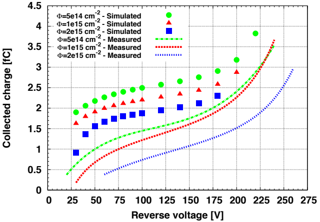

Charge multiplication (CM)

- Evidence of CM was found in irradiated planar and 3D detectors
- CM was observed in older generations of both FBK and CNM 3D detectors
  [A. Zoboli, et al., NSS08 Conf. Record, 2721]
  [M. Köhler, et al., NIMA659 (2011), 272]
- Triggered by high electric field at the tip of the junction columns
- Confirmed by numerical simulations
  [G. Giacomini, et al., VERTEX2011, POS]
- **Can charge multiplication be exploited?!?**

Motivation

- Increasing interest in reducing the total material budget
- Reduction of the sensor thickness
- Lower thickness $\rightarrow$ less detection volume
- Reduction in available charge for particle detection

Idea and investigation through numerical simulations

- A shrinking of all geometries by a factor of $\sim$3 will allow to also reduce inter-electrode spacing and column diameter
- Bulk thickness: $\sim$70 μm
- Column diameter: $\sim$4 μm
- Higher field at lower voltages

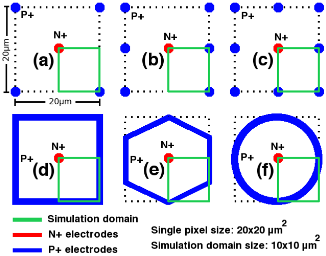

[M. Povoli, et al., submitted to NIMA (2013)]

Thin 3D detectors with built-in charge multiplication

Simulation results

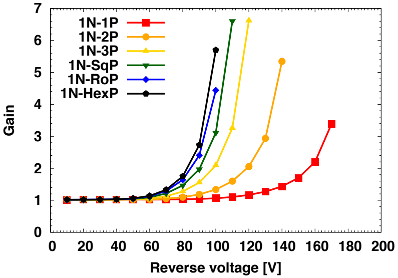

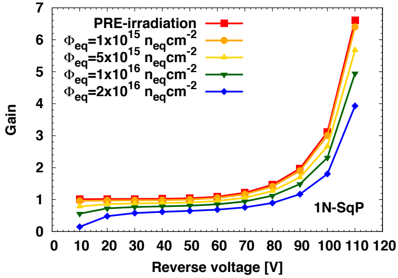

Gain before irradiation

- All investigated structures show CM
- The onset of CM changes with geometry
- Lower operating voltages for structures having trench ohmic electrodes
- A good gain uniformity was found within the entire investigated cell

Gain after HEAVY irradiation

- Results reported only for the rectangular cell
- Bulk radiation damage modeled with a 3 level trap model
- Reduction of the collected charge due to trapping (expected)
- **No change in CM onset voltage**
- **Completely recover charge trapping**

Thin 3D detectors with built-in charge multiplication

Surface isolation and electrode efficiency

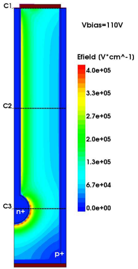

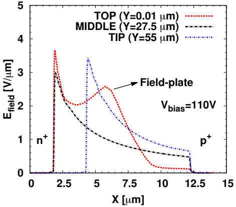

Final sensor geometry

- Rectangular cell shape
- P-spray and ~4 μm field-plate
- Raise the n^+ column to avoid critical regions on the backside
- Modification of the tip shape in order to avoid early breakdown phenomena
- Extracted 1D electric field profiles show that the surface and tip field are under control
- Possible to operate in CM mode

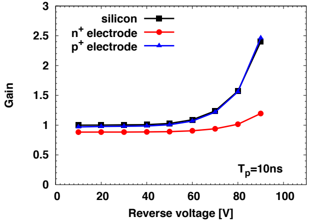

Electrode response

- Crucial to have polysilicon filling and sufficiently large lifetimes in it
- Lifetimes calibrated to match the electrode efficiency found for Stanford detectors

Full 3D MIP simulation (proposed shaping time of 10 ns)

- Three hit points investigated (bulk and both electrode types)
- CM properties similar to the simplified structure
- p^+ electrode is fully efficient and show good CM
- n^+ electrode is less efficient and shows lower CM
- Multiplication of the charge generated under the tip

HYbrid DEtectors for neutrons (HYDE)

Neutron detection

- Bare silicon is not able to detect neutrons
- Need for a converting material
- The most used converter is LiF
- Most of the commercial devices are able to only detect thermal neutron

Neutron detectors produced with 3D technology

- Purposely designed cavities
- Cavities are filled with the converter
- **Increased interaction probability between reaction products and silicon**

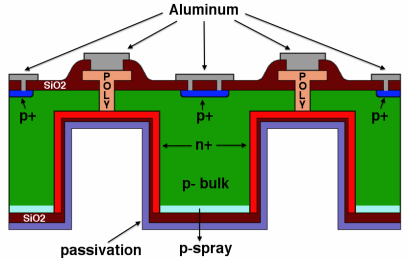

The HYDE project (INFN)

- Innovative polysiloxane converter
- Detects both thermal and fast neutrons
- Reaction products: **recoil protons** and **light** in the blue to red range

Realized detectors

- The cavities are connected through columnar pillars
- Both with an without polysilicon filling
- Good leakage currents and breakdown voltages
- The converter is deposited at Laboratori Nazionali di Legnaro

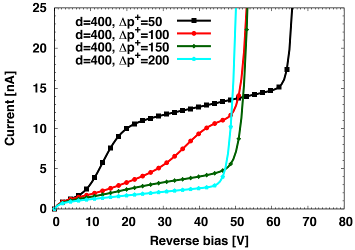

HYbrid DEtectors for neutrons (HYDE)

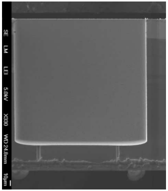

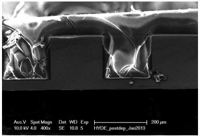

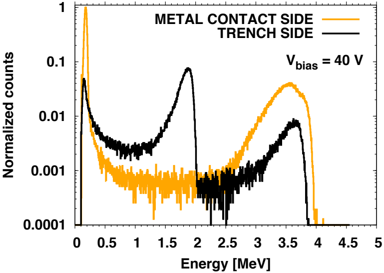

SEM pictures

- Fabricated cavity with connecting pillars (LEFT)
- The same after filling with converter (RIGHT)

α-particle measurements

- Measurements from both sides of the sensors
- Main peak correspond to ^{241}Am alphas (except for the energy loss in air)
- Lower peak from the trench side: geometrical motivations

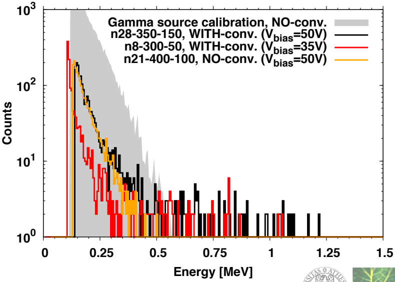

Neutron beam measurements

- Calibration with radioactive sources (α,γ)
- Bare sensor as comparison and two sensors with converter
- Indication of increased statistics in the range from 0.5 to 1.25 MeV (<u>VERY PRELIMINARY</u>)

CONCLUSIONS

- An enhanced 3D-DDTC sensor concept with fully passing through columns was designed at University of Trento and fabricated at FBK
- All the performed studies allowed to gain a better understanding of the behavior of 3D detectors both from the electrical and the functional point of views
- 3D Pixel detectors compatible with the FE-I4 readout chip proved to operate efficiently in IBL operating conditions
- These devices were chosen, together with CNM 3D detectors and planar 3D detectors, to populate the ATLAS Insertable B-Layer which will be installed during the first long shutdown of the LHC (2013-2014)
- The large amount of activities performed in the framework of the ATLAS 3D sensor collaboration triggered new ideas that are currently being investigated and will be soon tested

Thank you!